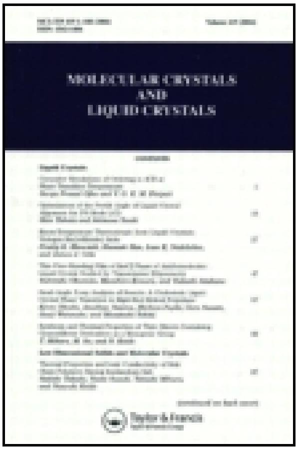

Molecular Crystals and Liquid Crystals
Publication details, including instructions for authors and subscription information:
http://www.tandfonline.com/loi/gmcl20

Liquid Crystal α,ω-Hexyl-Distyryl-Bithiophene: Morphology and Charge Tranport Properties in Organic Thin Film Transistors

Y. Didane [a] , C. Videlot-Ackermann [a] , H. Brisset [a] , J. Ackermann [a] , P. Raynal [a] , F. Fages [a] & G. H. Mehl [b]

[a] Ingénierie Moléculaire et Matériaux Fonctionnels, Centre Interdisciplinaire de Nanoscience de Marseille (CINaM), Aix Marseille Université, Campus Luminy, France
[b] Department of Chemistry, University of Hull, Hull, United Kingdom

Version of record first published: 05 Oct 2009

To cite this article: Y. Didane, C. Videlot-Ackermann, H. Brisset, J. Ackermann, P. Raynal, F. Fages & G. H. Mehl (2009): Liquid Crystal α,ω-Hexyl-Distyryl-Bithiophene: Morphology and Charge Tranport Properties in Organic Thin Film Transistors, Molecular Crystals and Liquid Crystals, 507:1, 178-187

To link to this article: http://dx.doi.org/10.1080/15421400903050715

Mol. Cryst. Liq. Cryst., Vol. 507, pp. 178–187, 2009
Copyright © Taylor & Francis Group, LLC
ISSN: 1542-1406 print/1563-5287 online
DOI: 10.1080/15421400903050715

Liquid Crystal α,ω-Hexyl-Distyryl-Bithiophene: Morphology and Charge Tranport Properties in Organic Thin Film Transistors

Y. Didane[1], C. Videlot-Ackermann[1], H. Brisset[1], J. Ackermann[1], P. Raynal[1], F. Fages[1], and G. H. Mehl[2]
[1]Ingénierie Moléculaire et Matériaux Fonctionnels, Centre Interdisciplinaire de Nanoscience de Marseille (CINaM), Aix Marseille Université, Campus Luminy, France
[2]Department of Chemistry, University of Hull, Hull, United Kingdom

*The solution and solid-state properties as well as the organic thin film transistor (OTFT) behavior of α,ω-hexyl-distyryl-bithiophene (***DH-DS2T***) are presented. Liquid Crystal properties were studied by differential scanning calorimetry (DSC) and optical polarising microscopy (OPM). High vacuum evaporated thin films were studied by optical absorption, scanning electron microscopy (SEM) and implemented as p-type semiconducting layers into organic thin film transistors (OTFTs).*

Keywords: liquid crystal; morphology; oligothiophene derivative; organic semiconductor; thin film transistor

1. INTRODUCTION

Over the last years, there has been a tremendously increasing interest in organic semiconductors [1]. Such materials find applications as active components in organic thin film transistors (OTFTs), solar cells and organic light-emitting diodes (OLEDs) [2]. OTFTs represent a

---

The authors acknowledge S. Nitsche for SEM pictures. C. V.-A. and F. F. gratefully acknowledge the "Agence Nationale de la Recherche" for supporting this work (grant ANR-06-BLAN-0295).

Address correspondence to C. Videlot-Ackermann or H. Brisset, Ingénierie Moléculaire et Matériaux Fonctionnels, Centre Interdisciplinaire de Nanoscience de Marseille (CINaM) CNRS-UPR-3118, Aix Marseille Université, Campus Luminy, Case 913, Marseille, Cedex 09 13288, France. E-mail: videlot@cinam.univ-mrs.fr or brisset@univmed.fr

conventional tool for studying charge-transport physics in conjugated compounds, but they also reached the point of now being viable in integrated circuit applications [3]. Indeed organic transistors are expected to play a major role in printed electronics for the fabrication of devices on flexible substrates. Nevertheless in order to ensure manufacturing costs as low as possible, such processes need to be carried out under ambient conditions, which require the materials and devices to be stable toward exposure to oxygen and moisture. Recently, we reported a new series of structurally simple and readily available oligothiophene derivatives end-capped with styryl units, **DSnT** ($n = 2$–4), that were used as the semiconducting layer in OTFTs [4]. The devices not only showed very high field-effect mobility (up to $0.1\,cm^2/Vs$) and on/off ratios (up to 10^5), but were also found to be exceptionally long-lived (more than one year of storage) and stable toward continuous operation, under atmospheric conditions. As these conjugated core were shown to lead to long-term stability, we thus decided to synthesize and investigate di-*n*-hexyl-terminated analogues [5]. The presence of the terminal alkyl chains should allow the introduction of new properties such as liquid crystal behavior and solubility in organic solvents. Soluble oligomers are a very promising and versatile class of materials for flexible electronics. When properly designed, these materials dissolve in common organic solvents and can be processed from liquid solution at room temperature. Such solutions are often called 'semiconducting inks' because they can be deposited and patterned using low-cost technologies such as inkjet, gravure, or offset printing.

We describe herein the solution and solid-state properties as well as the organic thin film transistor (OTFT) behavior of α,ω-hexyl-distyryl-bithiophene **DH-DS2T** (Fig. 1). The solid-state structural of thin films obtained by high-vacuum evaporation are presented depending on the surface treatment of Si/SiO_2 substrates and on the organic film thickness. In this contribution, the growth mode of **DH-DS2T** is studied in more details and optimized conditions are given that provided improved hole mobility compared to our previous report [5].

2. EXPERIMENTAL PART

The synthesis of **DH-DS2T** has been described previously [5]. The product was purified on a silica gel column eluting with a mixture methylene chloride-cyclohexane (1:4, v/v). The desired fractions were collected and evaporated to dryness to afford the *E* isomer. The total amount of product issued from the synthesis permitted to obtain a high quantity of pure **DH-DS2T** (1.5 g). Thermal properties were

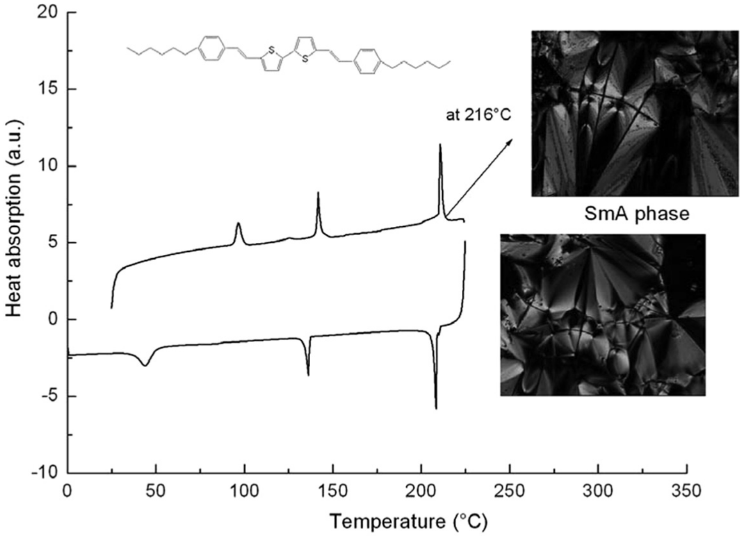

FIGURE 1 DSC scan of **DH-DS2T**. Insert: Images of focal conical defects of **DH-DS2T** at 216°C and chemical structure of **DH-DS2T**.

investigated using a Mettler Toledo differential calorimeter (DSC 822^e) in nitrogen against an indium standard. Transition temperatures were determined as the onset of the maximum in the endotherm or exotherm. The mesophases were studied on an Olympus BH-2 optical polarising microscope, equipped with a Mettler FP82 HT hot stage and a Mettler FP90 central processor. Pictures of the mesophases were taken using a JVC digital video camera connected to a PC. Software *Studio Capture*, supplied by Studio86Designs was used for image capturing. UV-visible absorption spectra were obtained on a Varian Cary 1E spectrophotometer.

The "top contact" configuration was used for the OTFT devices based on **DH-DS2T** oligomers. Highly n-doped silicon wafers (gate), covered with thermally grown silicon oxide SiO_2 (3000 Å, insulator layer), were purchased from Vegatec (France) and used as device substrates. Trimethylsilyl functionalization of the SiO_2/Si surface was carried out by dipping the silicon wafers to hexamethyldisilazane (HMDS) solution overnight at room temperature. The capacitance per unit area of either untreated or HMDS-treated silicon dioxide dielectric layers was $1.2–1.3 \times 10^{-8}\,F/cm^2$. Organic compound was vacuum deposited onto the substrates, using a Edwards Auto 306 apparatus, at a rate of 7 nm/min under a pressure of 1.6×10^{-6} mbar

TABLE 1 Charge Carrier Mobility (μ), On/Off Ratio and Threshold Voltage ($V_{t,}$) for OTFTs Based on **DH-DS2T** on Untreated and HMDS-Treated Silicon Oxide (SiO_2/Si) Substrates

Oligomer	Substrates	μ (cm^2/Vs)	On/Off	V_t (V)
DH-DS2T	SiO_2/Si	$3.4\text{–}4 \times 10^{-2}$	$3 \times 10^4\text{–}2.7 \times 10^6$	3–10
	HMDS-treated SiO_2/Si	$1.6\text{–}2.4 \times 10^{-2}$	$2 \times 10^4\text{–}2.4 \times 10^6$	1.6–5.4

to a nominal thickness of 55 nm as determined with a in situ quartz crystal monitor. The Au source and drain electrodes (channel length L = 25 or 50 μm, channel width W = 1 mm) were evaporated on top of the organic thin film through a shadow mask. Current-voltage characteristics were obtained at room temperature under ambient conditions with a Hewlett-Packard 4140B pico-amperemeter-DC voltage source. The source-drain current (I^D) in the saturation regime is governed by the equation:

$$(I_D)_{\mathrm{sat}} = (W/2L)\, C_i \mu (V_G - V_t)^2 \tag{1}$$

where C_i is the capacitance per unit area of the gate insulator layer, V_G is the gate voltage, V_t is the threshold voltage, and μ is the field-effect mobility. The on/off ratio values given in Table 1 were determined from the current I_D at $V_G = -100$ V to the current I_D at $V_G = +20$ V under a constant drain-source voltage $V_D = -30$ V. All the data in Table 1 were obtained by randomly measuring 3–5 individual OTFTs. Scanning electronic microscopy (SEM) pictures were realized by a JEOL field emission gun scanning electron microscope (FEG-SEM, model JSM 6320F).

3. RESULTS AND DISCUSSION

3.1. LC Characterization

The condensed state behaviour of the materials **DH-DS2T** was investigated by differential scanning calorimetry (DSC) and optical polarising microscopy (OPM) up to 300°C. **DH-DS2T** has a rich polymorphism with reversible crystalline transitions at 140°C and 210°C (Fig. 1). At this temperature the material melts into a SmA phase whose texture displays focal conical defects, as typically observed for a SmA phases (Fig. 1). This smectic phase is found stable up to 232.8°C where a phase transition to a nematic phase, characterized by a *Schlieren* and marbled texture, can be noticed. At 239.8°C

DH-DS2T melts into an isotropic liquid. The transitions are observable on reversing the temperature, however it is noted that the thermal stability of the material in the mesomorphic state is considerably lower than in the crystalline phase. Prolonged annealing in the LC state leads to degradation, detectable as a shift of the transitions to lower temperatures and a colour change of the material.

3.2. Optical Properties

The electronic absorption spectra of **DH-DS2T** in dichloromethane solution and in thin film vacuum deposited on quartz substrate are given in Figure 2. The spectrum in solution shows a broad 0–0 transition at 430 nm with vibronic shoulders at 407 and 455 nm suggesting a more rigid ground state geometry in the ground state as compared to parent oligothiophenes (nT) [6] where a broad transition without any shoulder is observed. The optical energy gap value (E_g) obtained by extrapolation of the low-energy edge of the UV-visible absorption spectra is 2.56 eV. The solid-state spectrum shows a drastically different behavior with the appearance of an intense and narrow peak at 342 nm together with a peak around 500 nm. This behavior is attributed to the exciton interactions between adjacent molecules in a closed-packed organization as obtained during vapour-deposition of organic molecules on substrate to form thin-films. Such a behavior

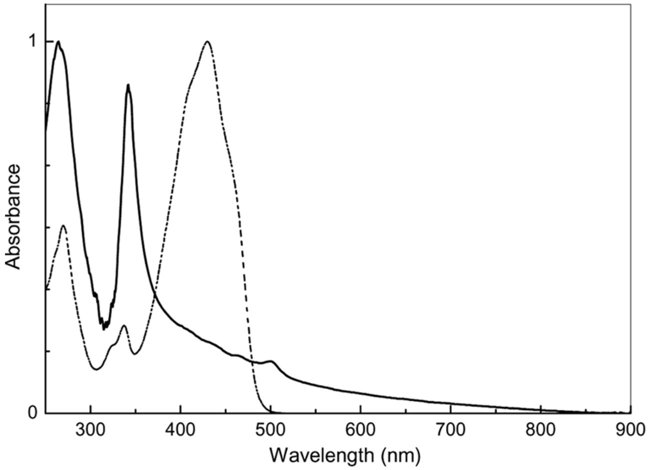

FIGURE 2 Electronic absorption spectra of **DH-DS2T** in dichloromethane solution (dotted line) and in thin film vacuum deposited on quartz substrate (full line).

confirms the strong coupling between π-conjugated systems in the solid state to form polycrystalline thin films as described in thin film morphology paragraph.

3.3. Thin Film Morphology

The morphology of organic thin films realized by vacuum evaporation can be influenced by different parameters such as the chemical structure of the organic molecule itself, the evaporation rate, the pressure, the temperature of substrates during the organic deposition and the nature of substrates. In order to evaluate the influence of the substrate, a dipping in HMDS solution of some silicon oxide (SiO_2/Si) substrates was realized. Deionised water was added dropwise at the volumes of about 2 μl onto the surface of horizontal untreated and HMDS-treated SiO_2/Si substrates using a microsyringe. Pictures of the droplets were acquired through a digital camera positioned on a static contact angle analyzer. Contact angle calculation was performed by applying the spherical approximation of the drop. The angle was obtained by estimating the tangent to the drop at its intersection with the surface of the substrate. Figures 3a and 3b give the shapes of a

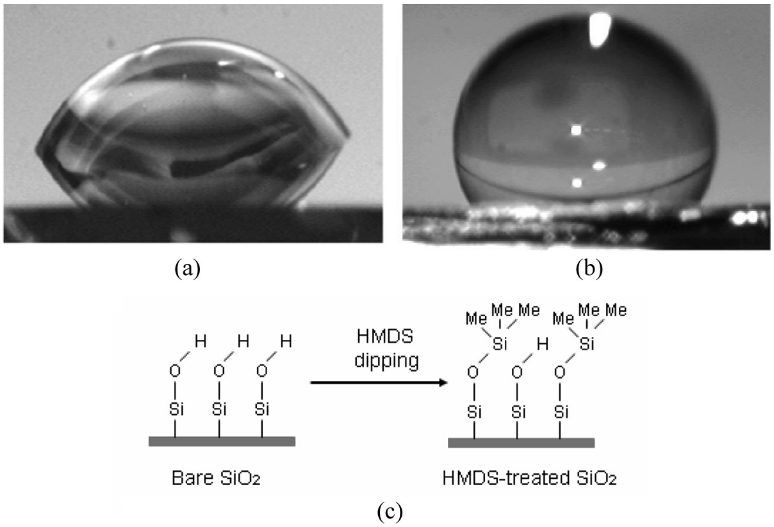

(a)

(b)

(c)

FIGURE 3 Shapes of a water droplet on an untreated (a) and a HMDS-treated (b) silicon oxide (SiO_2/Si) substrate. (c) Schematic representation of the chemical reaction occurring on the surface of SiO_2 substrates by dipping in HMDS solution.

water droplet on an untreated and a HMDS-treated silicon oxide (SiO_2/Si) substrate, respectively. The results reveal that the water contact angle increased abruptly from 55°–60° for bare SiO_2/Si to around 90° for HMDS-treated SiO_2/Si, indicating that the formation of a thin layer of HMDS on top of SiO_2 changed the surface from hydrophilic to hydrophobic. Figure 3c gives a schematic representation of the chemical reaction occurring on the surface of SiO_2 substrates by dipping in HMDS solution. Different chemical natures of the surface substrate prior organic vacuum deposition can induce different initial growth process. The morphology of vapor-deposited **DH-DS2T** films grown on untreated and HMDS-treated SiO_2/Si substrates was studied by SEM. Figure 4 gives SEM pictures of **DH-DS2T** thin films deposited on either untreated (Figs. 4a, 4c and 4e) or HMDS-treated (Figs. 4b, 4d and 4f) silicon oxide (SiO_2/Si) substrates. **DH-DS2T** thin films are deposited with a nominal thickness of 55 nm (Figs. 4a–4d) or 10 nm (Figs. 4e and 4f). On both substrates, **DH-DS2T** thin films formed large grains for which a terrace-and-step morphology can be noticed as shown in Figures 4c and 4d, together with needle like grains pointing out of the substrate. Nevertheless, **DH-DS2T** thin films on HMDS-treated SiO_2/Si substrates show larger crystalline grains on the surface. The needles like grains grown out of the substrate, which are morphological defects, are smaller. In the case of thinner films, both images (Figs. 4e and 4f) demonstrate a complete covering of the substrate surface by the first **DH-DS2T** monolayers as well as the beginning of the needle like grain formation. The surface is smoother in the case of HMDS-treated SiO_2/Si for 10 nm-thick film resulting from a better initial growth process via a layer-to-layer growth mode.

3.4. Organic Thin Film Transistors (OTFTs)

Top-contact thin film transistors of **DH-DS2T** oligomers were fabricated as described in the Experimental part. Drain and source Au electrodes were deposited on top of the semiconducting layer after the latter was evaporated onto untreated and HMDS-treated SiO_2/Si substrates. Figure 5a gives a schematic representation of the top contact configuration where the treatment layer based on HMDS is realized prior the organic deposition, while a top view of a canal ($L = 50\,\mu m$) between source and drain electrodes is given on Figure 5b. All measurements were performed in air at room temperature. Table 1 collects the electrical data in terms of mobility (μ), threshold voltage (V_t) and current on/off ratio (on/off) obtained with Eq. (1). Transistor responses were obtained only for negative bias, which is indicative

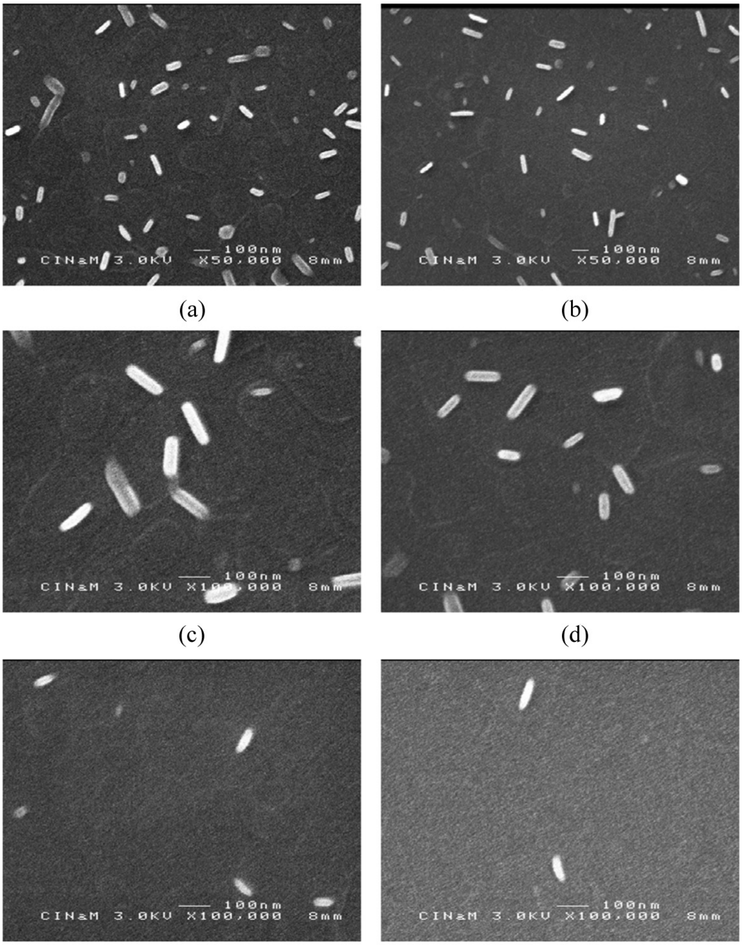

(a) (b)

(c) (d)

(e) (f)

FIGURE 4 SEM pictures of **DH-DS2T** thin films deposited on untreated (a, c, e) and a HMDS-treated (b, d, f) silicon oxide (SiO_2/Si) substrates. Film thicknesses are 55 nm for (a–d) and 10 nm for (e, f).

that **DH-DS2T** is a p-type semiconductor (Fig. 6). The devices work in the accumulation mode with the presence of a well-defined linear regime at $V_D < V_G$ followed by a saturation regime at $V_D > V_G$. Hole mobilities as high as $4 \times 10^{-2}\,cm^2/V \cdot s$ for OTFT devices elaborated at 30°C on SiO_2/Si substrates are achieved in air with a positive threshold voltage (V_t) of ~3–10 V. OTFTs based on **DH-DS2T** exhibit very high on/off ratio (up to 10^6) due to a concomitant low off state

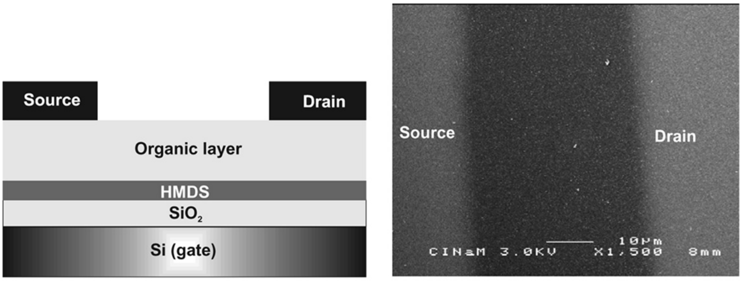

(a) (b)

FIGURE 5 Schematic "top contact" configuration used for OTFT measurements (a) and top view by SEM of an OTFT (b).

($I_D \sim 5 \times 10^{-12}$ A at +20 V) and a high on state ($I_D \sim 1.2 \times 10^{-5}$ A at −100 V). Higher mobility values are obtained to compare to the previous reported work [5] due to a higher purity of **DH-DS2T** compound. HMDS treatment was observed to decrease the threshold voltage V_t relative to unmodified samples due to a lower density of traps at the semiconductor/insulator interface in agreement with previous reports [7]. However, the average mobility decreases. This

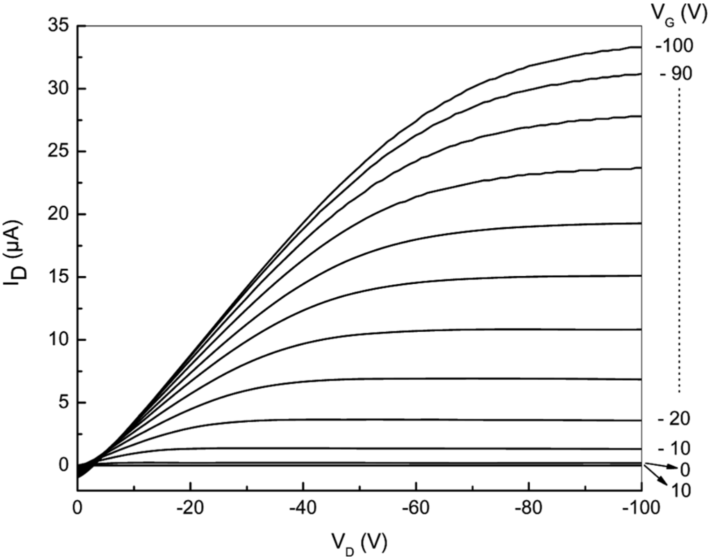

FIGURE 6 Output characteristic of an OTFT device fabricated on untreated SiO_2/Si with **DH-DS2T** as active layer.

observation points out that in the operation of OTFTs charge carrier transport is strongly dependent on the properties of the interface between the semiconductor and the insulator, i.e., the first organic monolayers deposited on the dielectric (SiO_2 or HMDS-SiO_2) surface. The physical contact between alkyl and HMDS chains has a dramatic influence on the device performance in terms of mobility and threshold voltage.

4. CONCLUSION

We have described the properties of a new oligothiophene derivative, α,ω-hexyl-distyryl-bithiophene (**DH-DS2T**), that behaves as a p-type semiconductor into organic thin film transistors (OTFTs). The presence of the terminal alkyl chains allows the introduction of new properties such as liquid crystal behavior and solubility in organic solvents.

REFERENCES

[1] Murphy, A. R. & Fréchet, J. M. J. (2007). *Chem. Rev.*, *107*, 1066.

[2] (a) (2004). For a recent account on organic electronics, see the special issue of *Chemistry of Materials*: *Chem. Mater.*, *16*(23); (b) Dimitrakopoulos, C. D. & Malefant, P. R. L. (2002). *Adv. Mater.*, *14*, 99.

[3] (a) Sirringhaus, H., Tessler, N., & Friend, R. H. (1998). *Sciences*, *280*, 1741; (b) Sirringhaus, H., Tessler, N., & Friend, R. H. (1999). *Synthetic Metals*, *102*, 857; (c) Sheraw, C. D., Zhou, L., Huang, J. R., Gundlach, D. J., Jackson, T. N., Kane, M. G., Hill, I. G., Hammond, M. S., Campi, J., Greening, B. K., Francl, J., & West, J. (2002). *Appl. Phys. Lett.*, *80*, 1088; (d) Fix, W., Ullmann, A., Ficker, J., & Clemens, W. (2002). *Appl. Phys. Lett.*, *81*, 1735.

[4] Videlot-Ackermann, C., Ackermann, J., Brisset, H., Kawamura, K., Yoshimoto, N., Raynal, P., El Kassmi, A., & Fages, F. (2005). *J. Am. Chem. Soc.*, *127*, 16346.

[5] Videlot-Ackermann, C., Brisset, H., Ackermann, J., Zhang, J., Raynal, P., Fages, F., Mehl, G. H., Tnanisawa, T., & Yoshimoto, N. (2008). *Organic Electronics*, *9*, 591.

[6] Fichou, D. (Ed.), (1999). *Handbook of Oligo- and Polythiophenes*, Wiley-VCH: Weinheim, Germany.

[7] Gojanc, T. C., Lévesque, I., & D'Iorio, M. (2004). *Appl. Phys. Lett.*, *84*, 930.